The FAUST Framework: Free-Form Annotations on Unfolding Vascular Structures for Treatment Planning

Patrick Saalfeld, Sylvia Glaßer, Oliver Beuing, Bernhard Preim

The FAUST Framework: Free-Form Annotations on Unfolding Vascular Structures for Treatment Planning

Patrick Saalfeld[a], Sylvia Glaßer[a], Oliver Beuing[b], Bernhard Preim[a]

[a]*Department of Simulation and Graphics, University of Magdeburg, Germany*
[b]*Department of Neuroradiology, University Hospital Magdeburg, Germany*

Abstract

For complex interventions, such as stenting of a cerebral aneurysm, treatment planning is mandatory. Sketching can support the physician as it involves an active involvement with complex spatial relations and bears a great potential to improve communication. These sketches are employed as direct annotation on 2D medical image data and print outs, respectively. Annotating 3D planning models is more difficult due to possible occlusions of the complex spatial anatomy of vascular structures. Furthermore, the annotations should adapt accordingly to view changes and deforming structures.

Therefore, we developed the FAUST framework, which allows creating 3D annotations by freely sketching in the 3D environment. Additionally to generic annotations, the physician is supported to create the most common treatment options with sketching single strokes only. We allow an interactive unfolding of vascular structures with adapting annotations to still convey their meta information. Our framework is realized on the zSpace, which combines a semi-immersive stereoscopic display and a stylus with ray-based interaction techniques.

We conducted a user study with computer scientists, carried out a demo session with a neuroradiologist and assessed the performance. The user study revealed a positive rating of the interaction techniques and a high sense of presence. The neuroradiologist stated that our framework can support treatment planning and leads to a better understanding of anatomical structures. Our performance evaluation showed that our sketching approach is usable in real-time with a large number of annotations. Furthermore, our approach can be adapted to a wider range of applications including medical documentation.

Keywords: 3D Sketching, Annotations, Semi-immersive Environments, Treatment Planning, Vascular Structures

1. Introduction

For clinical treatment planning, physicians need to obtain a spatial understanding of the patient's anatomy and pathologies [1]. Parameters such as shape, volume and spatial relationships of structures have to be considered [2]. Software assistants support the physician in medical practice to reliably and efficiently carry out special tasks [3]. Such medical issues comprise access planning, resection and implant planning. Here, the assisting software may provide the possibility to annotate pathologic variations and visualize treatment options [1, 4]. Such sketched annotations are beneficial to communicate and elaborate complex treatment strategies without the necessity to draw precisely and accurately [5]. However, annotations on 3D image data are usually drawn image-based [6], which causes problems when physicians change the view and annotations do not adapt accordingly. A common solution is recalculating the position in the image domain [7], which introduces difficulties during relocation of annotations reasoned by disturbing non-continuous motions [8]. Furthermore, a mental and algorithmic combination of the 3D model and the image domain comprising the annotations has to be carried out. In our FAUST framework, we allow to create annotations directly in object space as 3D sketches. Hence, we bring together 3D sketching with computer-assisted surgery planning. We *pin* the annotations to the 3D model. Thus, our annotations still convey their meta information on dynamic medical data, such as time-varying or unfolding data. 3D sketches are usually used and appreciated in product design [9, 10, 11], which takes advantage of stylists' skills, acquired through training over time [9]. However, for physicians the annotation of medical structures in 3D with complex treatment options can be laborious and includes the risk of not achieving the desired result. Therefore, our FAUST framework assists the physician in different ways:

- the physician can create generic annotations as well as the most common treatment options by sketching and combining center lines only,
- an optional geometric constraint that allows for a direct projection of the sketch on the surface model,
- a semi-immersive system combining a stereoscopic display with head tracking to support depth perception, and
- the 3D sketching, realized with a six degrees of freedom (6DoF) stylus and ray-based interaction techniques.

Email address: saalfeld@isg.cs.uni-magdeburg.de

We decided to use the semi-immersive 3D User Interface (3DUI) *zSpace* instead of a fully immersive system, because it is less intruding to the typical workflow of a physician but still provides important depth cues such as motion and binocular parallax.

As an example of a spatially complex vascular structure, we chose the *Circle of Willis* (CoW), which comprises a circular combination of arteries supplying the brain and surrounding structures (see Figure 1). Beneath the clinical importance, the CoW is well suited for our approach for two reasons. First, it includes many different sub-structures, which results in a variety of access paths and treatment options. The possibility to freely annotate supports the visualization of different treatment plans. Second, the CoW is represented either in its real, self-occluding 3D anatomical state or as a simplified 2D illustration. To maintain a mental representation of both states including annotations, an interactive and seamless transition can support the physician.

The evaluation of our framework has three parts. First, we conduct a user study to reveal usability problems and to quantify the sense of *presence*. Presence is a measure to assess immersion, and thus, an indicator of how beneficial the semi-immersive system is. Second, we carry out an intensive demonstration session and unstructured interview with an experienced neuroradiologist. Third, we assess different performance aspects, i.e., the necessary calculation time to attach annotations to the CoW as well as the frame rate during interaction and unfolding. The average ratings of the interaction techniques, usability and presence yield positive ratings. The results of our interview indicate that our framework improves the spatial overview of vascular structures and supports the understanding of anatomical structures compared to angiographic 2D images. Regarding the performance evaluation, we achieve real-time frame rates for the attachment of annotations and during interaction with a high number of annotations.

Our paper is organized as follows: **Section 2** provides a short medical background. Here, the CoW is described in more detail and a medical application scenario is motivated based on an interview with a neuroradiologist. **Section 3** summarizes related work in the fields of annotations in combination with sketch-based interfaces, unfolding of medical data and animation of 3D structures. In **Section 4**, the preprocessing steps to convert the medical data in a planning model are described. Based on this model, the unfolding procedure is explained. **Section 5** presents our FAUST framework containing input and output devices as well as interaction techniques. **Section 6** summarizes the evaluation, **Section 7** discusses challenges to integrate the framework into clinical routine and **Section 8** concludes our paper.

2. Medical Background and Application Scenario

Diagnosis and treatment of cerebrovascular diseases is a frequent and challenging task in clinical practice. The treatment of cerebral vessels requires in-depth knowledge of patient-individual morphology. The central part of the cerebral vessel system is the CoW (see Figure 1). It comprises a circular combination of arteries supplying the brain and surrounding structures. Its formation allows for bypassing the blood flow in case of a blocked artery. However, the anatomical manifestation of the arteries underlies strong, patient-specific variations with respect to shape and length [13]. Furthermore, there are several CoW configurations where some arteries are underdeveloped or completely missing. Therefore, the CoW is an excellent example for the challenging and complex 3D anatomy.

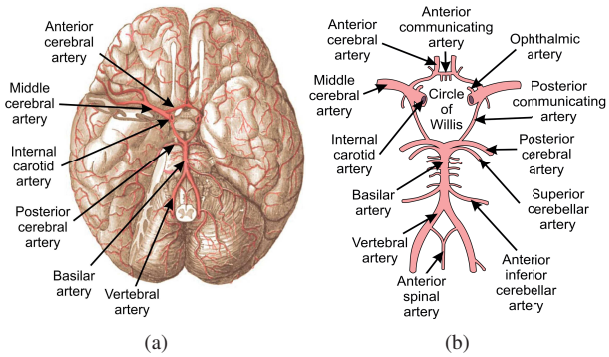

Figure 1: The blood supply of the brain is maintained by the anterior and the posterior cerebral circulation (a) and the CoW (b) as backup circulation (adapted from illustrations from Gray [12]).

For an in-depth understanding of our application scenario, we interviewed a neuroradiologist (co-author of this paper) with more than 20 years of professional experience. We stated questions regarding endovascular treatment of cerebral aneurysms, i.e., saccular dilatations of cerebral arteries. Regarding the cause of aneurysms, some risk factors are identified. For example, in 10 % of the cases, the afflicted patients have a genetic predisposition. Aneurysms bear an annual chance of 1 % to actually rupture [14], resulting in death or permanent disability in more than 40 % of the cases [15]. Overall, approximately 2 % to 5 % of the entire population is affected by cerebral aneurysms [14, 16]. Treatment is usually carried out via *surgical clipping* or *endovascular therapy*. The first one aims at a closure of the aneurysm neck with a clip. Endovascular therapy includes the deployment of stents and flow diverters, which redirect the cerebral blood flow yielding a decreased blood flow in the aneurysm. Another therapy is endovascular coiling, where small wires are placed inside the aneurysm to promote blood clotting and a possible occlusion of the aneurysm. Stenting and coiling are also be used in combination. The choice of treatment is based on several criteria, e.g., location, shape and size of the aneurysm. Furthermore, treatment methods vary in aspects such as the used access path as well as different clip sizes, stent lengths and coil types. We account for the huge variety of different parameters and configurations by letting the physician sketch freely, and thus, allow him to take into account even special cases.

An example for such a special case are unruptured aneurysms with increased neck sizes. The large neck sizes are not suited for plain or balloon-assisted coiling. They frequently require stenting to protect the parent vessels permanently. Even

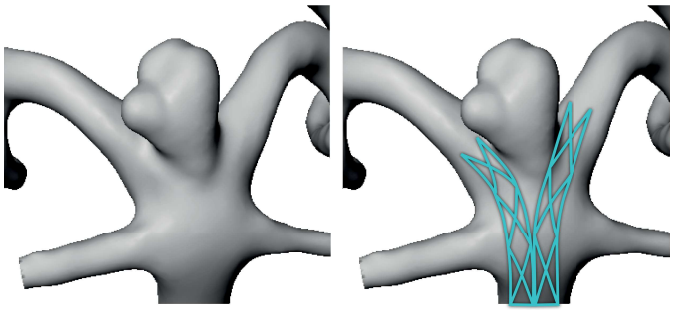

Figure 2: Illustration of Y-stenting, where two stents are inserted.

two stents may be necessary in aneurysms arising at a bifurcation. Here, Y-. X- or T-stenting procedures are performed (see Figure 2). For Y-shaped stents (also called *kissing stents*), two guide wires are carefully positioned such that the two stents can be released alternatingly. Therefore, the patient-individual anatomy must be analyzed, which often involves the acquisition of 3D digital subtraction images to overcome superimposition in the 2D angiography image data. Special care is required to prevent hampering of the blood supply by blocking branching arteries. Furthermore, both stents should end at the same position and should be adapted to the patient-individual vessel diameter. To further reduce the aneurysm's inflow and to promote blood clotting and a possible closure, coils are deployed after the Y-stenting. The treatment planning involves a thorough evaluation of the patient-specific CoW's spatial anatomy. More important, the aneurysm and the direct surroundings have to be analyzed.

We developed the FAUST framework to support the clinician with free-form sketching. With the possibility of 3D annotations, various options are considered, e.g., different stent configurations, coil lengths and access paths. The framework also favors the evaluation of patient-specific spatial anatomy and can reveal branching arteries.

3. Related Work

This section comprises related work of labels as a form of annotations in immersive environments as well as sketch-based interfaces. Additionally, we describe how curved structures from medical image data are unfolded. Lastly, animations are discussed for a seamless blending of structures from their original, curved shape to a flattened one.

Annotations in medicine are primarily used as textual labels to support education [17]. They are either visualized as internal labels on the structure's surface or beneath them as external labels [18]. Recently, labeling approaches were used in immersive environments. Tatzgern et al. [19] use automatically placed labels in an augmented reality to annotate 3D structures with images and texts. Nowke et al. [20] use automatically placed labels in a CAVE (cave automatic virtual environment). In contrast, an *interactive positioning* of labels avoids the usage of a complex label layout algorithm, but introduces challenges regarding user interaction. An example of interactively placed annotations is the work from Assenmacher et al. [21]. They present a framework for various types of annotations including different input and output metaphors. The comparison of Madsen et al. [8] shows that directly placing annotations in object space instead of image space leads to the best performance for label location tasks. Our goal is not only to locate existing annotations, but also to create them in object space.

Sketching is related to labels in terms of enriching medical data with meta information. For example, sketching is used as an intuitive interaction technique to annotate medical reports [6] or to segment structures in 2D image data [22]. In clinical practice, sketching is also an easy supplement for patient education or interchange with the medical staff. Another possibility is using *Sketch-based Interfaces for Modeling* (SBIM) [23] to directly create medical structures, e.g., branching vessels with integrated blood flow [24]. Fleisch et al. [9] describe a *3D sketching* environment and try to close the gap between 2D sketching and 3D modeling in an immersive environment for designers. They present techniques for creating and modifying 3D curves, such as stroke splitting and oversketching. Saalfeld et al. [25] use a semi-immersive environment to sketch different vascular structures for medical education. Wang et al. [26] and Jackson et al. [27] combine 2D sketching and an immersive environment. The former work allows freehand sketching for cartoonists on a virtual, user-definable 3D canvas, i.e., the user is restricted to a virtual plane. The latter work allows users to import existing 2D sketches and interactively *lift* 2D curves into space to create 3D structures. In our previous work, we presented the concept to sketch treatment methods directly on 3D structures [28]. Perkunder et al. [11] investigated differences of 2D and 3D sketching for modeling in a study. There, sketching in a 3D environment was perceived more stimulating and attractive than under 2D conditions.

Curved tubular structures, such as blood vessels, bronchi or the colon, are of high interest in medicine. For the assessment of these structures, tomographic image data is acquired. However, the necessary information rarely lies in a single image plane, which motivates the unfolding of these structures. An established technique for this limitation is *Curved Planar Reformation* (CPR) [29]. Here, the center line of the tubular structure is derived and flattened. The flattened structure is then mapped into a new, single image providing its longitudinal view. There exist several adaptations of the CPR which focus on specific structures. For example, Williams et al. [30] introduced an extension which is suitable for large, hollow structures such as the trachea or the colon. To investigate the whole tubular structure with these two methods, the visualization has to be rotated around the central axis. An approach to aggregate these rotated images in one image was suggested by Mistelbauer et al. [31]. All these techniques allow a depiction of the unfolded structures in an additional 2D view. However, the task to mentally transfer the distorted unfolded image to the 3D volume rendering view is left to the physician. Neugebauer et al. [32] solved this by embedding a 2D projection of a cerebral aneurysm surface as contextual information around the 3D visualization. Another approach is used by Vilanova et al. [33]. They integrate the unfolding directly into the 3D volume rendering by using the center line of a colon to flatten it for virtual endoscopy. Our so-

lution is based on this idea. However, instead of visualizing the unfolded structure only, we allow the physician to seamlessly blend between the original and unfolded 3D representation in an animated, interactive manner.

To visualize the seamless transition of the original to the unfolded representation, animations may be used. In general, there are two possibilities to represent the animation of 3D meshes: keyframe and skeletal animations [34]. In *keyframe animations*, several sequences of the same but deformed mesh are stored. For the animation, the sequences are played consecutively. This approach is memory-intensive since each mesh has to be loaded during animation. Furthermore, the final result depends on the amount of keyframes, which have to be hand-crafted in a time-consuming process. Therefore, we use skeletal animation, which strongly simplifies the animation procedure and is supported by a wide range of development frameworks. In *skeletal animation*, the original surface representation is provided with a skeleton represented by a set of interconnected bones. As a skeleton, the center line can be employed. Here, each line segment of the center line becomes a bone of the skeleton. In contrast to keyframe animation, the vertices of the surface are not animated directly. Instead, in a process called *skinning*, every vertex is assigned to one or multiple bones with a specific weight. The weight determines how strongly each bone influences a specific vertex. Now the bones are animated and the vertices are transformed accordingly. The results can lead to intersection and distortion artifacts. These are addressed with different approaches, e.g., representing the surface implicitly, calculate the deformations for the implicit representation and transfer the results back to the geometry [35]. The work of Chaudhry et al. [36] compares different techniques regarding efficiency and realism. In our work, we unfold from a folded state and, thus, no intersection artifacts occur.

4. Material

This section describes the process to transform the 3D medical image data of the CoW into a surface model. Afterwards, the workflow to create the animated unfolding vessel is described. The whole process is illustrated in Figure 3.

4.1. Reconstruction of the 3D Surface Mesh

We extract the CoW from a healthy patient's MRI data set which was acquired for clinical education using the MAGNETOM Skyra 3T (Siemens Healthcare GmbH, Erlangen, Germany) combined with a 20-channel-head/neck coil with a voxel resolution of $.26\,mm \times .26\,mm \times .5\,mm$. For the 3D surface mesh extraction, we follow the procedure describe by Glaßer et al. [37]. The mesh was extracted with MeVisLab, a rapid prototyping tool for medical image processing (Fraunhofer MEVIS, Bremen, Germany) by applying a threshold-based segmentation. Subsequently, we smoothed the extracted triangular surface mesh with Sculptris (Pixologic, Los Angeles, U.S.A.) and cutted off unnecessary outlets with Blender (Blender foundation, Amsterdam, the Netherlands). After that, we artificially modeled an aneurysm and a stenosis based on real clinical patient data. The generated pathologies were approved by an interventional neuroradiologist.

4.2. Unfolding of the Reconstructed Mesh

As discussed in Section 3, we use skeletal animation for the unfolding. Normally, the skeleton consists of a hierarchical set of connected bones. However, the reconstructed CoW is a closed surface with a genus of one, i.e., it has a hole, an automatic procedure to create a center line would result in a cyclic graph instead of a hierarchy. Therefore, we create the animation manually with 3ds Max (Autodesk, Inc., California, U.S.A). We first create multiple skeletons and attach them to the reconstructed CoW (Fig. 3). After skinning, we manually unfold the skeletons with a combination of forward and inverse kinematics. This process allows us to pay particular attention to prevent strong deformations. Now, we define two keyframe states: one in the original folded state and the second in the unfolded state. We animate the unfolding by interpolating between these two keyframes (Fig. 4). In character animation, the limbs of the initial mesh are normally spread apart, which eases the rigging and skinning process and reduces deformations during animations. This is different for the CoW due to its initial folded state. Yet, the thereby introduced deformations are acceptable even for medical treatment planning. This is due to the fact that the unfolded structure primarily supports the physician to illustrate vessel transitions and spatial relationships, which are persistent even in the unfolded structure. For the original, folded structure, anatomical correctness is required, but this structure is not affected by the deformations.

5. Annotation of Unfolding Vascular Structures

This section comprises details about the used hardware of our 3DUI. Next, the free-form annotations are described, including technical realization aspects, different types of annotations and their visualization. After that, the illustration possibilities of the CoW are explained and the used interaction techniques are described, including the animated unfolding. Our framework is developed with the game engine Unity (Unity Technologies, San Francisco, U.S.A.).

5.1. Input and Output Device

We decided to use the semi-immersive zSpace (zSpace Inc., San Francisco, U.S.A.) system for our FAUST framework. It combines binocular and motion parallax in a fish tank environment, which are important depth cues to support the physician in estimating sizes and relationships of anatomical structures [38]. Fish tank environments are in particular suitable in scenarios where the user manipulates the virtual world from *outside in* and the size of the virtual object is smaller than the user's body [39], which applies for the CoW. The zSpace's stereoscopic display renders full HD with 120 Hz. The binocular parallax is achieved with circular polarized rendered images for passive glasses. The glasses are tracked through infrared (IR) markers with 6DoF and enable motion parallax. As input

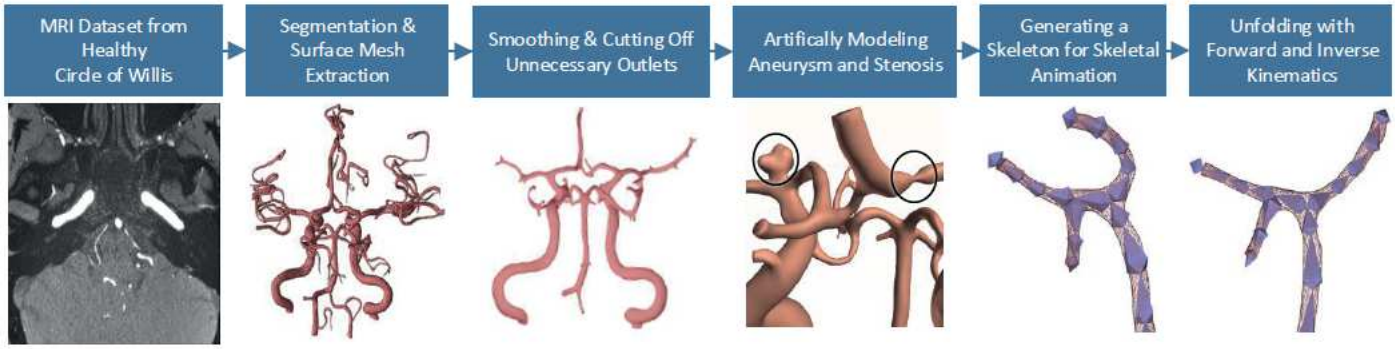

Figure 3: Workflow to create the unfolding Circle of Willis from Magnetic Resonance Images (MRI).

Figure 4: Overview of the animated unfolding from orthographic top (1st row), orthographic left (2nd row) and perspective 3D (3rd row).

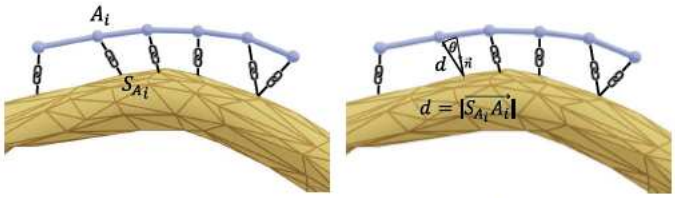

Figure 5: To link the annotation to the surface, for each annotation point A_i the closest surface vertex S_{A_i} is determined by searching in a kd-tree (a). Then, the relative position consisting of a rotation angle θ and the distance d is stored. The annotation point A_i maintains these two properties during unfolding of the Circle of Willis.

device, a stylus connected to the zSpace is used which is tracked with IR LEDs and allows 6DoF interaction. The orientation of the stylus is virtually extended into the rendered scene and is represented as a visible ray to enable ray-based interaction.

5.2. *Creating and Attaching Annotations*

The free-form annotations are created with equidistantly resampled points from the stylus. These points are linked to the 3D surface. Thus, they adapt their position and shape during the unfolding of the CoW. To link the points of the annotation to the surface, for each annotation point A_i the closest surface vertex S_{A_i} is used. To find S_{A_i} in an efficient way, we store all vertices of the surface in a kd-tree. However, the interactive unfolding changes the position of the surface's vertices. Therefore, an adjustable amount of kd-trees in different unfolding states is generated and stored in a list. If the user starts annotating, the current unfolding state is compared with states in the list. The most similar state and, thus, kd-tree is selected. Now, a relative description between A_i and S_{A_i} is necessary. First, the distance $d = |\overrightarrow{S_{A_i}A_i}|$ is calculated. Then, the angle between the normal $\vec{n}$ from S_{A_i} and the vector $\vec{v} = \overrightarrow{S_{A_i}A_i}$ is calculated as $\theta = \angle(\vec{n}, \vec{v})$ and stored as a quaternion. During unfolding, we ensure that this relative description, i.e., the distance d and θ are maintained. This process is illustrated in Figure 5.

Since this attachment is computationally expensive, the number of annotation points is critical. However, a reduced amount of points leads to a visual unpleasing representation of annotations. In general, the amount of sample points could be reduced by discarding points which do not contribute to the general shape, e.g., with the Douglas-Peucker Algorithm [40]. However, such approaches are not appropriate for our scenario due to the animated unfolding inducing a non-rigid change of the annotation shape. Therefore, we equidistantly resample the points. This is realized by discarding all points which exhibit a distance to their neighbors that falls below a certain threshold t. If the user moves the stylus very fast, this threshold is exceeded. In this case, additional points are generated between the last and newest point. This fast and simple resampling method is only problematic if either the threshold t is too large and, thus, no detailed annotations can be sketched or if the sampling rate is too low during fast sketching. We empirically determined t by sketching coils, which are the thinnest structures and require the most details. Since our framework allows real-time sketching with this threshold, the first problem is addressed. To assess the sampling rate of the stylus in combination with sketching speed, we sketched several annotations in fast speed. Here, we measured a covered distance of approximately 19 cm/s. The stylus is tracked with 100 Hz, i.e., a sampling point is created around every 19 mm. This distance is sufficient for annotations with low curvature, e.g., stents and access paths. For annotations with higher curvature, the physician usually pays particular attention on details and, therefore, sketches with less lower speed.

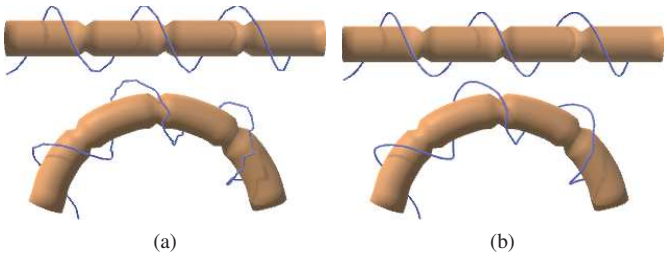

(a) (b)

Figure 6: The illustration shows a bended tubular shape surrounded by a spiral free-form annotation. The distortion of the annotation during bending is shown for no smoothing (a) and 5-neighborhood Gaussian smoothing (b).

During the unfolding, undesired effects could hamper the visualization of the sketches, i.e., a sketched straight line in the unfolded state could result in a zig-zag line in the folded state. To weaken this effect, we smooth the visual representation of the annotation points with 5-neighborhood Gaussian smoothing (Fig. 6).

5.3. Types and Visualization of Annotations

The user can create three different types of annotations: generic annotations, stents and coils. This differentiation is chosen based on typical tasks in treatment planning. Stents and coils are the most common treatment options. For heterogeneous tasks, such as highlighting important regions and illustrating access paths, our generic annotations are a flexible tool to sketch different configurations. For all types, we procedurally generate a cylindrical surface mesh along the sketched line in real-time. This allows us to support depth perception by applying shading techniques to the 3D surface. Furthermore, the radius of the cylindrical surface can be adjusted. Thus, the user can sketch stents with varying diameters for different vessels or thin coils inside an aneurysm. To aid the user in the process of sketching, annotations can be constrained to lay on the planning model's surface. This helps to, e.g., illustrate an access path along a vessel. For the *generic annotations*, the user can choose between four different colors. All colors are rendered with an illustrative cel-shading [41] to support visual differentiation between the CoW and generic annotations. A silhouette further improves the contrast between the vessel structure and background. To annotate the vascular structure with *stents*, we applied a grid texture to the cylindrical surface. By using the alpha channel of the texture, the user is able to look through the struts, which results in a realistic stent illustration. Here, x and y texture coordinates are necessary. These are calculated during sketching by increasing the x-coordinate along the sketched path. The y-coordinate is mapped around the 360 degrees of the cylinder. For *coils*, a brushed metal texture is applied with the same approach. Additionally, metal shading properties are applied to the shader. All sketching types are shown in Figure 7.

5.4. Visualization of the Vascular Structures

The CoW is visualized with a physically-based rendering to obtain a realistic surface representation. This technique simulates the behavior of light more realistically. For example, the idea of energy conservation is used, e.g., less light is reflected than received, specular light minimizes the diffuse amount of light and a Fresnel effect is added (the surface becomes more reflective at grazing angles) [42]. This representation is further improved with a texture. In contrast to the annotations, the texture coordinates cannot be calculated directly, since the vessel and its branches can be arbitrarily located. A time-consuming approach to set these coordinates is to create them in a 3D modeling application. We choose an automatic approach from procedural terrain modeling, i.e., tri-planar texture mapping [43]. Here, the normal of each vertex is mapped to a texture on the x-, y-, and z-plane. The resulting color is a weighted combination of the three texture colors. This weight depends on the amount the normal is facing in one of the directions. For example, if the normal is facing exactly to the z-direction, only the color of the x-y-plane would be taken into account. The same technique is used for a normal map to give the impression of depth on the vascular surface. To allow the users to draw inside the CoW, we let them choose between two visualizations: a fully opaque one and a shading technique which reveals the inside of the vessel. In Figure 8, the two visualization techniques with and without texture and normal mapping are depicted.

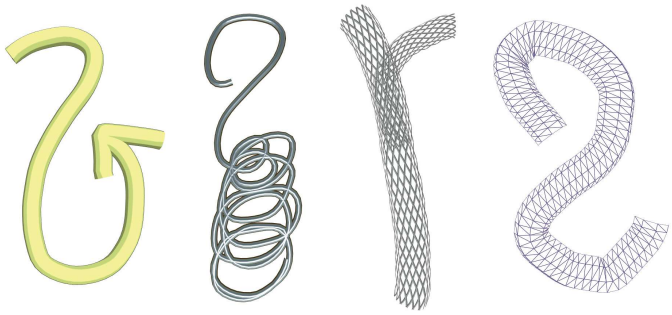

Figure 7: An overview of different annotation types from left to right: generic yellow annotation, coil, stent. The last image shows the wireframe of our procedurally generated cylinder.

5.5. Interaction Techniques

5.5.1. Translation and Rotation

The interaction technique to translate and rotate objects commonly used (e.g., by all shipped zSpace demonstrations) is a direct ray-based one. There, the stylus is virtually extended into the scene. By pressing a stylus button, the object is pinned to the virtual ray. Now, every stylus movement results in a translation and rotation of the CoW. Although this interaction technique was understood immediately in our user tests, participants had problems to rotate the CoW accurately. Therefore, we decoupled translation and rotation by triggering each transformation with a different stylus button (Fig. 9). If the translation button is pressed, the position of the virtual ray tip T is used to calculate the stylus' movement delta $\vec{m}$ with $\vec{m} = \overrightarrow{T_{start}T_{end}}$. The object is then translated by the amount of $\vec{m}$. For rotation, we used the Arcball 3D technique, since it was preferred when it was compared to direct interaction in a study conducted by Katzakis et al. [44]. Here, the structure is surrounded by an invisible sphere. The intersection point P_i of the ray and the

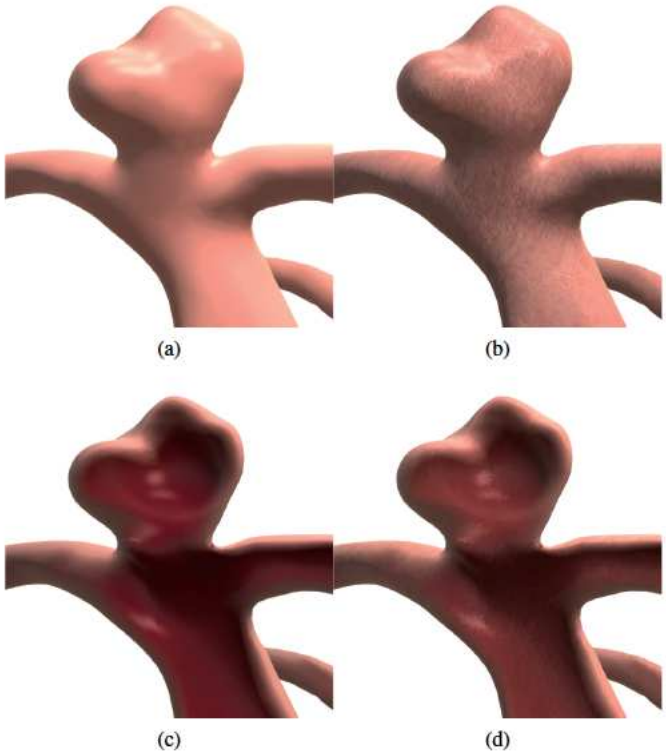

Figure 8: The physician can choose between a opaque (a, b) and semi-transparent (c, d) visualization of the vascular structure. To improve the visualization, we applied a texture and bump map to the surface via tri-planar texture mapping (b, d).

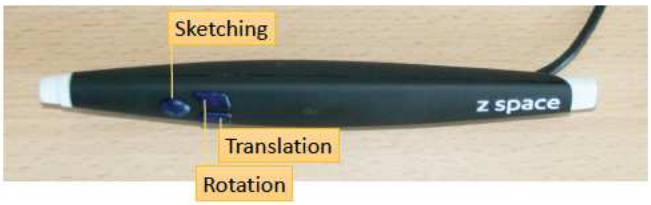

Figure 9: The zSpace's stylus with the assigned functions to the different buttons.

sphere surface is used to calculate the rotation delta α. If the rotation button is pressed, the vector $\vec{v_1}$ is determined with the sphere center S_c as $\vec{v_1} = \overrightarrow{S_c P_i}$. During movement of the stylus, the new vector $\vec{v_2} = \overrightarrow{S_c P_{iNew}}$ is calculated. The rotation axis $\vec{R}$ is extracted as $\vec{v_1} \times \vec{v_2}$ and the rotation angle α is defined as $\alpha = \angle \vec{v_1} \vec{v_2}$. The translation and rotation are illustrated in Figure 10.

To support the physician maintaining an overview of the CoW's orientation, a torso with synchronized orientation is visualized in the right bottom corner (see Figure 11). Additionally, the physician can reset the view by pressing a button that restores the initial frontal view.

5.5.2. *Animated Unfolding*

For the animation of the unfolding CoW, a slider widget is used (Fig. 11). The value of the slider is mapped to 0 and 1, representing the two keyframe states (0: original and folded,

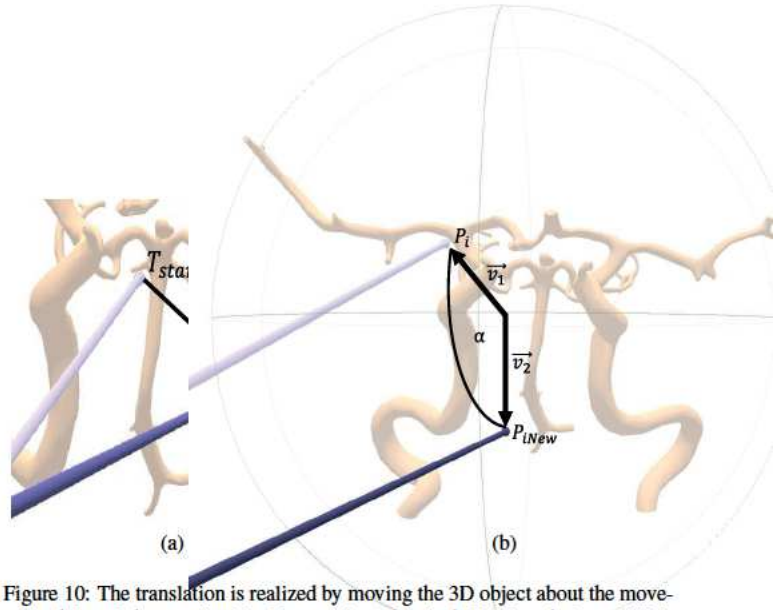

Figure 10: The translation is realized by moving the 3D object about the movement delta of the ray tip (a). For rotation, the Arcball 3D technique [44] is used, where the rotation is derived from the ray intersection with an invisible bounding sphere (b).

1: unfolded, recall Section 4.2) of the skeletal animation generated in 3ds Max. If the slider value is changed, the position and orientation of every skeleton's bone is interpolated to this value, resulting in a transforming CoW. The value is continuously approached over time to guarantee a smooth transition without abrupt changes of the unfolding state.

Figure 11: A screenshot of the FAUST framework. On the left, the physician can choose between different annotation and visualization types, constrain the sketches to the surface and reset the view. The interactive unfolding is realized with the slider widget at the bottom. The torso at the right bottom illustrates the current orientation of the Circle of Willis.

5.6. *Using the FAUST Framework for a Y-Stenting Procedure*

A possible sequence to plan the Y-stenting procedure with our framework is illustrated in Figure 12. The physician starts by investigating the vascular structures and highlighting pathologies with generic annotations (Fig. 12a). Then, the access paths have to be defined. Here, a completely unfolded CoW allows an easier 3D sketching. Additionally, the annotations are constrained to lie on the surface (Fig. 12b). Now, the Y-stent is placed to treat the aneurysm with a large neck size. Two stents have to be placed with different diameters (Fig. 12c). Finally, the physician reduces the aneurysm inflow by sketching thin coils inside the aneurysm (Fig. 12d).

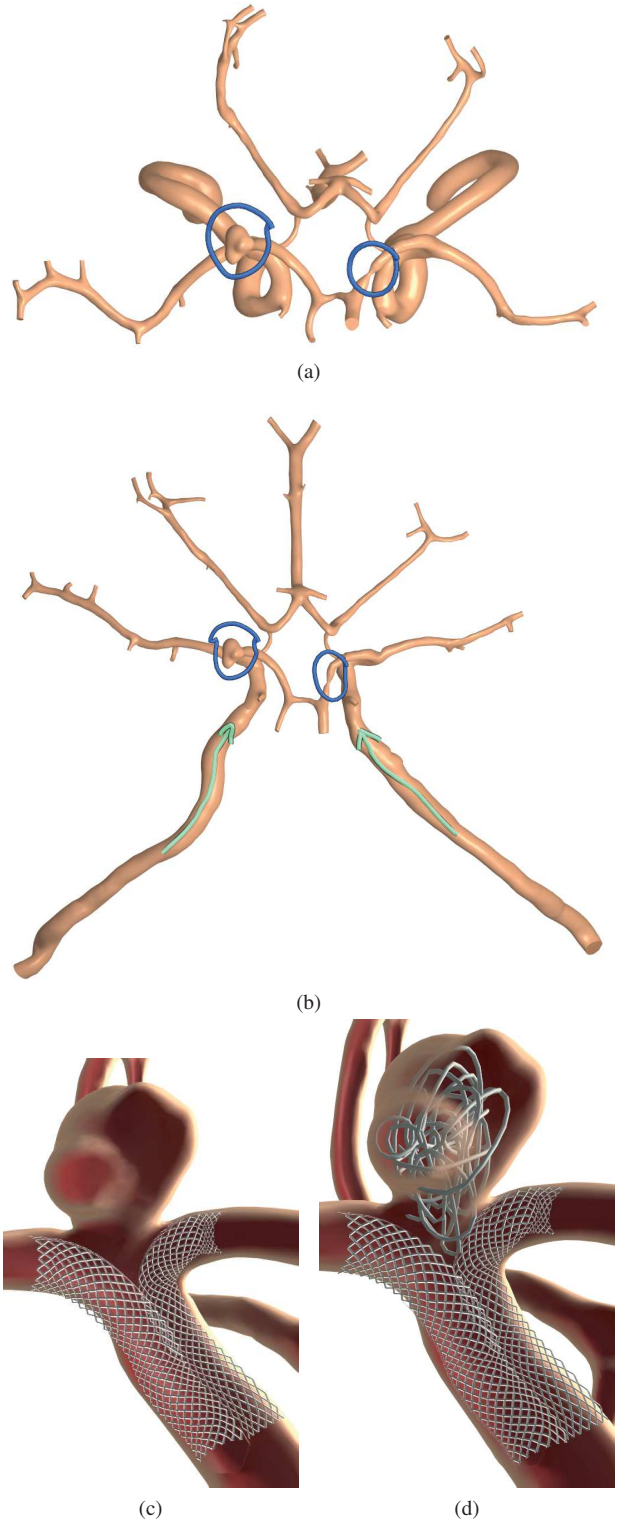

Figure 12: The images illustrate a possible treatment planning of the Y-stenting procedure. In (a) pathologies (an aneurysm and stenosis) of the Circle of Willis are highlighted with generic annotations. The unfolded CoW is depicted in (b). Two possible access paths are sketched on the vascular surface. In (c), the transparent visualization is used to allow the physician to sketch inside. A Y-stent is sketched in the splitting arteries under the aneurysm. The final step of treatment planning, i.e., placing the coil inside the aneurysm, is shown in (d).

6. Evaluation

Since our FAUST framework is designed for a specific medical application, the number of potential participants is limited. Additionally, the special hardware setup would not allow, e.g., a web-based study. Therefore, we decided to plan our user evaluation in two steps:

1. Computer scientists (no one is co-author of this paper) with advanced knowledge on vascular systems used our framework to sketch different annotations. Even if these users are no physicians, gaining information about usability and technical aspects of the framework is possible.
2. We performed an demo session and unstructured interview with a potential expert user (co-author of this paper), i.e., an experienced neuroradiologist. Here, the possible benefits achieved with our framework are evaluated.

Finally, we evaluate the performance by measuring the calculation time to attach annotations as well as the frame rate drop caused by adding annotations.

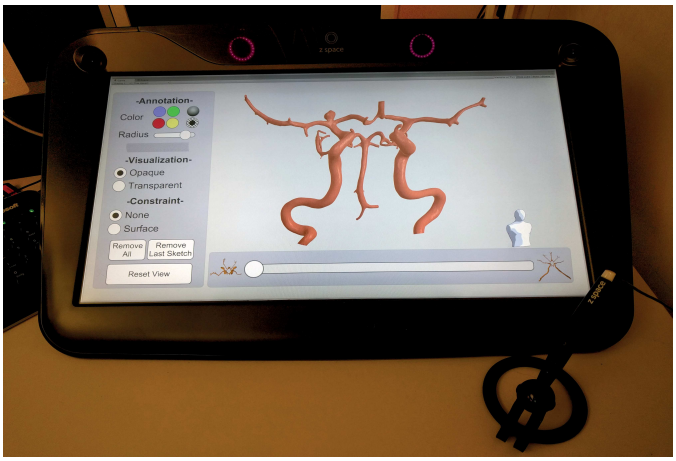

Figure 13: The setup for our user study: the 3DUI zSpace and our running FAUST framework.

6.1. User Study

All computer scientists that participated in our user study had basic medical background knowledge on the human vascular system, most common pathologies (aneurysms and stenoses) and treatment options (coiling, clipping and stenting). However, they were unfamiliar with the advanced Y-stenting procedure and the particularities of the CoW (recall Section 2). To account for this, we started our evaluation with an introduction to the vascular system of the CoW, highlighting the stenosis and aneurysm in our CoW surface, as well as describing the Y-stenting to treat the aneurysm. Then, we introduced each participant to the FAUST framework, including a training of interaction techniques to translate, rotate and unfold the CoW followed by an explanation of the 3D sketching. After the training session, we asked each participant to use our framework to plan different treatment options, i.e., sketch access paths and a

Table 1: Years of participants' experience in domains related to our framework ($\bar{x}$ – mean, s – standard deviation).

	min	*max*	$\bar{x}$	s
Exp. with Medical Applications	1	12	3.9	3.5
Exp. with Scientific Visualization	0	12	4	3.6
Exp. with 3DUIs	0	3	1.2	1

clipping, stenting and coiling procedure. Finally, the treatment planning for Y-stenting of the aneurysm of our CoW was performed.

During the training and treatment planning, the participants were asked to think aloud. After the demo session, a questionnaire was handed out which consisted of three parts:

1. a demographic part including questions regarding years of experience in the field of medical applications, scientific visualization and 3DUIs,
2. questions regarding the usability and user comfort of the unfolding and sketching, as well as
3. the presence questionnaire from Witmer and Singer [45] which quantifies aspects such as realism and the quality of the interface. This questionnaire allowed us to understand the benefit achieved through the zSpace. Some questions did not match our framework, e.g., questions regarding sound or haptic feedback. Hence, these were left out.

The questions of part (2) and (3) were stated with a 7-point Likert scale.

6.1.1. Results

Nine participants took part in our study (one female, eight males) with an age between 26 and 38 ($\bar{x}$ (mean) = 28.8). The experience of our participants in different domains is represented in Table 1.

Although the participants had very little experience with 3DUIs ($\bar{x}$ = 1.2 years) compared to medical applications ($\bar{x}$ = 3.9 years), the rating of the interaction techniques was overall positive. This is in particular relevant since a similar experience ratio can be expected by physicians. The simplicity and plausibility of the unfolding were rated with *md* (median) = 3 (*min* = 2, *max* = 3). The question *how naturally the sketching is* was rated with a *md* = 2 (*min* = 0, *max* = 3). This result is promising, since 3D sketching bears the risk to be complicated due to the introduced third dimension. For the presence questionnaire, we combined the questions into the pre-defined categories: *Possibility to Act* (PA), *Realism* (R), *Possibility to Examine* (PE), *Quality of Interface* (QI) and *Self-evaluation of Performance* (SE). The results are summarized in Figure 14. All categories were positively rated, which supports our intention to use the zSpace to make the representation of the CoW more realistic and tangible. The lowest result was achieved in the category QI. The participants had difficulties to locate the stylus tip during the first annotations, which resulted in misplaced annotations. Their comments confirm that this is the reason why QI was rated lower than the other categories.

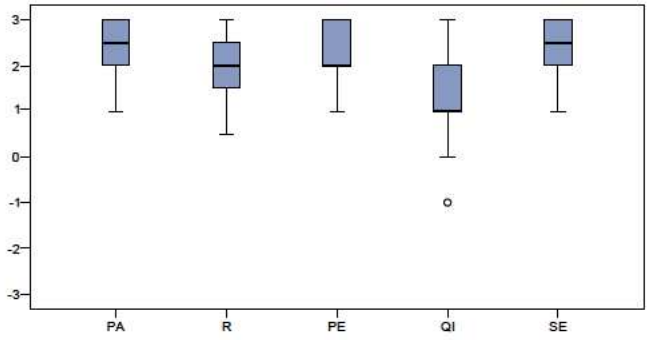

Figure 14: Boxplots summarize the results for different categories of the presence questionnaire [45]: Possibility to Act (PA), Realism (R), Possibility to Examine (PE), Quality of Interface (QI), Self-evaluation of Performance (SE). All categories were rated positively by the majority of our participants. For the categories PA, PE and SE, not all whiskers are visible, since the upper quartile is equal to the maximum. The circle in the category QI marks an outlier.

Five participants commented positively on the representation of the sketches. They stated that the shading supports shape perception and is visually pleasing. Further positive aspects mentioned by the participants are the realistic appearance of the CoW due to shading and fish tank VR as well as the intuitive control of the slider widget. The problems of the first misplaced annotations could be addressed by projecting a shadow of the stylus ray to a plane below the CoW.

6.2. Unstructured Interview

The unstructured interview was performed with the neuroradiologist, who supported us in defining our application scenario (recall Section 2). The setup of the interview is similar to the user study, except that the medical introduction was left out.

6.2.1. Results

The physician highlighted the several benefits:

- The sketching works well to describe access paths. The unfolded view supports this even more, because lines to describe the path could be sketched more easily.
- The unfolded state gives a spatial overview of the vascular structure and transitions, which is more difficult in 2D displays.
- The framework supports getting a better understanding of anatomical structures, e.g., the size of the aneurysm neck or the location of small branching vessels. This helps during interventions where the angiographic 2D images lead to occlusion.
- For Y-stenting, it is necessary that both stents end at the same position. Here, the original folded structure could be used to mark this position. The following unfolding supports the estimation of the necessary length of the stents.

Additionally to that, the neuroradiologist suggested additional features to improve our framework and pointed out drawbacks.

For example, a tool to allow the measurement of vessel diameters would be helpful. Furthermore, the combination of several sketches to realize complex spatial structures is difficult to achieve. He suggested a feature which allows to snap on old sketches or merge points which are close to each other.

6.3. Performance

For the performance evaluation we used the same desktop computer as in our user study. It is equipped with an Intel Core i7-2600K (3.7 GHz), 16 GB RAM and a Nvidia Quadro 4000. The most calculation-intensive steps in our framework are the attachment of annotations to the CoW and their non-rigid transformations during unfolding. Each annotation consists of a sequence of connected control points. The number of these points is essential for the performance. However, statements regarding their quantity without considering the resulting annotations would be meaningless. Therefore, we sketched several annotations and counted the control points. To create stents, generic annotations and coils, in average 30, 40 or 250 control points are necessary. Thus, for one annotation approximately $(30 + 40 + 250)/3 = 107$ control points are used.

To quantify the performance, we logged the time that is necessary to attach 107 control points on our CoW mesh with 33653 vertices and 65514 triangles. This took on average 151 ms. Since the attachment is performed after the physician finishes sketching, this time is almost unnoticeable. Additionally, we analyzed the frame rate of our framework during interaction and unfolding. Initially, FAUST runs with 30 frames per second (FPS). We measured the frame rate after adding control points in steps of 500. The performance drop was around 1 FPS every 500 control points, i.e., at 2000 added control points, 25 FPS were achieved. With 4500 control points, the framework runs at 20 FPS. FAUST is impractical to use below 15 FPS, which happens if more than 7000 control points are used. Using the approximated control point number of an annotation, this means $7000/107 = 65$ annotations could be added until the framework is unusable. Our tests and interview with the neuroradiologist show, that not even one third of 65 annotations is used, i.e., our framework runs at usable frame rates for treatment planning.

7. Integration into Clinical Practice

To introduce our framework into clinical practice, several aspects have to be considered. The most important ones are:

1. the acquisition costs,
2. available space,
3. familiarization to the 3D display, glasses and ray-based interaction techniques as well as
4. the time pressure in clinical routine.

We discussed these issues with our clinical partners. The acquisition costs of the zSpace are moderate compared to other hardware in interventional radiology. If available space is problematic, the zSpace display is usable as a normal 2D display and, thus, can replace the existing one used for treatment planning. The polarized glasses are the most invasive component, since they darken the view of the physician. This would be problematic during interventions; for planning alone, it is acceptable. Regarding the familiarization aspect, innovations in interventional radiology are common. Therefore, neuroradiologists are used to invest learning time for new technology. The fundamental precondition for this is that the introduced technology is beneficial for the patient, e.g., regarding risk minimization during interventions. The same argument applies for the time pressure during clinical routine. If the framework supports patient safety, this is more important than short planning times. To assess these aspects, we have to evaluate this in further studies. Considering the general possibility to fit in additional planning, this is possible for either elected and critical cases. For elective cases, where sufficient planning time is available, the treatment usually starts with medication for several days before an intervention. In this period, our Faust framework can be used for treatment planning. Even for critical cases, where an aneurysm is ruptured, it is not unusual to observe the patient overnight and start with treatment the next day. Even in this period, the application of our framework is possible.

8. Conclusion

Complex structures, such as patient-individual vessel trees with pathologies, require an excellent knowledge of the spatial variations and the 3D extent. At the example of the CoW with two pathologies, we investigated the possibility to support physicians in treatment planning. Our FAUST framework allows to freely create 3D sketches and, thus, enables the physician to annotate structures with a wide variety of different treatment options. Through our interactive unfolding, the whole CoW can be investigated at once and occlusions can be resolved. Conventional imaging cannot depict the same information, e.g., digital angiography yields a projection image with superimpositions and tomographic image data is not sufficient for assessing bended vessel structures.

The evaluation with computer scientists and a neuroradiologist indicates the usability of our interaction techniques as well as the usefulness of our framework for treatment planning.

Our FAUST framework was evaluated with the application of cerebral aneurysms, but it can be adapted to a wide range of complex anatomical structures, including treatment of vascular diseases in general or an unfolding colon. Here, other dynamic data can be used, such as time varying data of a beating heart. For future work, we want to investigate the usage of our framework in the area of patient documentation. The possibility to preserve a wide variety of annotations together with a 3D representation of the structure could greatly improve documentation.

Acknowledgment

This work was partially funded by the *German Federal Ministry for Economic Affairs and Energy* (grant number 'ZF4028201BZ5') and the *German Federal Ministry of Education and Research* within the research campus *STIMULATE* (grant number '13GW0095A').

References

[1] Preim B, Botha CP. Visual Computing for Medicine: Theory, Algorithms, and Applications. San Francisco, CA, USA: Morgan Kaufmann Publishers Inc.; 2013.

[2] Rössling I, Cyrus C, Dornheim L, Boehm A, Preim B. Fast and Flexible Distance Measures for Treatment Planning. International Journal of Computer Assisted Radiology and Surgery 2010;5(6):633–46.

[3] Klein J, Friman O, Hadwiger M, Preim B, Ritter F, Vilanova A, et al. Visual computing for medical diagnosis and treatment. Computers & Graphics 2009;33(4):554 –65.

[4] Krüger A, Kubisch C, Strauß G, Preim B. Sinus Endoscopy - Application of Advanced GPU Volume Rendering for Virtual Endoscopy. IEEE Transactions on Visualization and Computer Graphics 2008;14(6):1491–8.

[5] Jorge J, Samavati F. Sketch-based Interfaces and Modeling. Springer London; 2011.

[6] Reiner B, Siegel E. Radiology Reporting: Returning to Our Image-Centric Roots. American Journal of Roentgenology 2006;187:1151–5.

[7] Hartmann K, Götzelmann T, Ali K, Strothotte T. Metrics for Functional and Aesthetic Label Layouts. In: Proc. of Smart Graphics. Springer-Verlag; 2005, p. 115–26.

[8] Madsen JB, Tatzqern M, Madsen CB, Schmalstieg D, Kalkofen D. Temporal Coherence Strategies for Augmented Reality Labeling. IEEE Trans Vis Comput Graph 2016;22(4):1415–23.

[9] Fleisch T, Brunetti G, Santos P, Stork A. Stroke-input methods for immersive styling environments. In: Proc. of Shape Modeling and Applications. 2004, p. 275–83.

[10] Israel J, Wiese E, Mateescu M, Zöllner C, Stark R. Investigating three-dimensional sketching for early conceptual designresults from expert discussions and user studies. Computers & Graphics 2009;33(4):462 –73.

[11] Perkunder H, Israel JH, Alexa M. Shape modeling with sketched feature lines in immersive 3d environments. In: Proc. of Sketch-Based Interfaces and Modeling. 2010, p. 127–34.

[12] Gray H, Lewis WH. Anatomy of the Human Body. Philadelphia, Lea & Febiger; 1918.

[13] Kayembe KN, Sasahara M, Hazama F. Cerebral Aneurysms and Variations in the Circle of Willis. Stroke 1984;15(5):846–50.

[14] Ujiie H, Sato K, Onda H, Oikawa A, Kagawa M, Takakura K, et al. Clinical analysis of incidentally discovered unruptured aneurysms. Stroke 1993;24(12):1850–6.

[15] Bederson JB, Connolly ES, Batjer HH, Dacey RG, Dion JE, Diringer MN, et al. Guidelines for the Management of Aneurysmal Subarachnoid Hemorrhage: A Statement for Healthcare Professionals From a Special Writing Group of the Stroke Council, American Heart Association. Stroke 2009;40(3):994–1025.

[16] Vlak MH, Algra A, Brandenburg R, Rinkel GJ. Prevalence of unruptured intracranial aneurysms, with emphasis on sex, age, comorbidity, country, and time period: a systematic review and meta-analysis. Lancet Neurol 2011;10(7):626–36.

[17] Oeltze-Jafra S, Preim B. Survey of Labeling Techniques in Medical Visualizations. In: Proc. of Eurographics Workshop on Visual Computing for Biology and Medicine (EG VCBM). 2014, p. 199–208.

[18] Götzelmann T, Ali K, Hartmann K, Strothotte T. Form follows function: Aesthetic interactive labels. In: Proc. of Computational Aesthetics in Graphics, Visualization and Imaging. 2005, p. 193–200.

[19] Tatzgern M, Kalkofen D, Grasset R, Schmalstieg D. Hedgehog Labeling: View Management Techniques for External Labels in 3D Space. In: IEEE Virtual Reality. 2014, p. 27–32.

[20] Nowke C, Schmidt M, van Albada SJ, Eppler JM, Bakker R, Diesrnann M, et al. VisNEST - Interactive analysis of neural activity data. In: IEEE Symposium on Biological Data Visualization. 2013, p. 65–72.

[21] Assenmacher I, Hentschel B, Ni C, Kuhlen T, Bischof C. Interactive Data Annotation in Virtual Environments. In: Proc. of Eurographics Conference on Virtual Environments. 2006, p. 119–26.

[22] Heckel F, Moltz JH, Tietjen C, Hahn HK. Sketch-Based Editing Tools for Tumour Segmentation in 3D Medical Images. Computer Graphics Forum 2013;32(8):144–57.

[23] Olsen L, Samavati FF, Sousa MC, Jorge JA. Sketch-based modeling: A survey. Computers & Graphics 2009;33(1):85 – 103.

[24] Saalfeld P, Baer A, Preim U, Preim B, Lawonn K. A Sketch-Based Interface for 2D Illustration of Vascular Structures, Diseases, and Treatment Options with Real-Time Blood Flow; vol. 598; chap. Computer Vision, Imaging and Computer Graphics Theory and Applications: International Joint Conference, Revised Selected Papers. Springer International Publishing; 2016, p. 19–40.

[25] Saalfeld P, Stojnic A, Preim B, Oeltze-Jafra S. Semi-Immersive 3D Sketching of Vascular Structures for Medical Education. In: Proc. of Eurographics Workshop on Visual Computing for Biology and Medicine (EG VCBM). 2016, p. 123–32.

[26] Wang M, Fei G, Xin Z, Zheng Y, Li X. 3d freehand canvas. In: Proc. of Technologies for E-Learning and Digital Entertainment. 2008, p. 602–12.

[27] Jackson B, Keefe DF. Lift-Off: Using Reference Imagery and Freehand Sketching to Create 3D Models in VR. IEEE Trans Vis Comput Graph 2016;22(4):1442–51.

[28] Saalfeld P, Glaßer S, Beuing O, Grundmann M, Preim B. 3D Sketching on Interactively Unfolded Vascular Structures for Treatment Planning. In: IEEE Symposium on 3D User Interfaces (3DUI). 2016, p. 267–8.

[29] Kanitsar A, Fleischmann D, Wegenkittl R, Felkel P, Gröller ME. CPR: Curved Planar Reformation. In: Proc. of IEEE Visualization. 2002, p. 37–44.

[30] Williams D, Grimm S, Coto E, Roudsari A, Hatzakis H. Volumetric curved planar reformation for virtual endoscopy. IEEE Transactions on Visualization and Computer Graphics 2008;14(1):109–19.

[31] Mistelbauer G, Morar A, Varchola A, Schernthaner R, Baclija I, Köchl A, et al. Vessel Visualization Using Curvicircular Feature Aggregation. Computer Graphics Forum 2013;32(3):231–40.

[32] Neugebauer M, Gasteiger R, Beuing O, Diehl V, Skalej M, Preim B. Map Displays for the Analysis of Scalar Data on Cerebral Aneurysm Surfaces. In: Computer Graphics Forum (EuroVis); vol. 28 (3). 2009, p. 895–902.

[33] Vilanova Bartroli A, Wegenkittl R, Konig A, Groller E. Nonlinear virtual colon unfolding. In: Proc. of IEEE Visualization. 2001, p. 411–579.

[34] Lobao AS, Evangelista BP, Grootjans R. Beginning XNA 3.0 Game Programming: From Novice to Professional. 1st ed.; Berkely, CA, USA: Apress; 2009.

[35] Vaillant R, Barthe L, Guennebaud G, Cani MP, Rohmer D, Wyvill B, et al. Implicit Skinning: Real-time Skin Deformation with Contact Modeling. ACM Trans Graph 2013;32(4):125:1–125:12.

[36] Chaudhry E, Bian S, Ugail H, Jin X, You L, Zhang JJ. Dynamic skin deformation using finite difference solutions for character animation. Computers & Graphics 2015;46:294 – 305.

[37] Glaßer S, Hoffmann T, Voß S, Klink F, Preim B. Extraction of Patient-Specific 3D Cerebral Artery and Wall Thickness Models from 2D OCT and Structured-Light 3D Scanner Data. In: Proc. of German Society of Computer- and Robot-Assisted Surgery (CURAC). 2016, p. 197–202.

[38] Baer A, Hübler A, Saalfeld P, Cunningham D, Preim B. A Comparative User Study of a 2D and an Autostereoscopic 3D Display for a Tympanoplastic Surgery. In: Proc. of Eurographics Workshop on Visual Computing for Biology and Medicine (EG VCBM). 2014, p. 181–90.

[39] Demiralp C, Jackson CD, Karelitz DB, Zhang S, Laidlaw DH. CAVE and Fishtank Virtual-Reality Displays: A Qualitative and Quantitative Comparison. IEEE Transactions on Visualization and Computer Graphics 2006;12(3):323–30.

[40] Douglas DH, Peucker TK. Algorithms for the Reduction of the Number of Points Required to Represent a Digitized Line or its Caricature. Cartographica: The International Journal for Geographic Information and Geovisualization 1973;10(2):112–22.

[41] McGuire M, Fein A. Real-time Rendering of Cartoon Smoke and Clouds. In: Proc. of International Symposium on Non-photorealistic Animation and Rendering. 2006, p. 21–6.

[42] Pharr M, Humphreys G. Physically Based Rendering, Second Edition: From Theory To Implementation. Morgan Kaufmann Publishers Inc.; 2010.

[43] Nguyen H. Gpu Gems 3. Addison-Wesley Professional; 2007.

[44] Katzakis N, Seki K, Kiyokawa K, Takemura H. Mesh-Grab and Arcball-3D: Ray-based 6-DOF Object Manipulation. In: Proc. of Asia Pacific Conference on Computer Human Interaction. 2013, p. 129–36.

[45] Witmer BG, Singer MJ. Measuring Presence in Virtual Environments: A Presence Questionnaire. Presence: Teleoperators and Virtual Environments 1998;7:225–40.